

The CHIME FRB population do not track the star formation history of the universe

RACHEL C. ZHANG^{1,2} AND BING ZHANG³

¹*Center for Interdisciplinary Exploration & Research in Astrophysics (CIERA), Evanston, IL 60202*

²*Department of Physics & Astronomy, Northwestern University, Evanston, IL 60202*

³*Department of Physics and Astronomy, University of Nevada, Las Vegas, Las Vegas, NV 89154*

ABSTRACT

The redshift distribution of fast radio bursts (FRBs) is not well constrained. The association of the Galactic FRB 200428 with the young magnetar SGR 1935+2154 raises the working hypothesis that FRB sources track the star formation history of the universe. The discovery of FRB 20200120E in association with a globular cluster in the nearby galaxy M81, on the other hand, casts doubts on such an assumption. We apply the Monte Carlo method developed in a previous work to test different FRB redshift distribution models against the recently released first CHIME FRB catalog in terms of their distributions in specific fluence, inferred isotropic energy, and external dispersion measure (DM_E). Our results clearly show that the hypothesis that all FRBs track the star formation history of the universe is ruled out. The hypothesis that all FRBs track the accumulated stars throughout history describes the data better but still cannot pass both the energy and DM_E criteria. The data seem to be better modeled with either a redshift distribution model invoking a significant delay with respect to star formation or a hybrid model invoking both a dominant delayed population and an insignificant star formation population. We discuss the implications of this finding for FRB source models.

Keywords: fast radio bursts – radio transient sources – magnetars

1. INTRODUCTION

The engines that power cosmological fast radio bursts (FRBs) are not well identified. Different types of engines may follow different redshift distributions (e.g. Fig.1 of Zhang et al. (2021)), so constraints on the FRB redshift distribution would offer clues to the origins of FRBs. The discovery of the Galactic FRB 200428 in association with an X-ray burst from the magnetar SGR 1935+2154 (CHIME/FRB Collaboration et al. 2020; Bochenek et al. 2020; Li et al. 2021; Mereghetti et al. 2020; Ridnaia et al. 2021; Tavani et al. 2021) suggests that at least some FRBs originate from young magnetars produced from deaths of massive stars. As a result, the working hypothesis that the majority of FRB sources follow the star formation history of the universe has been widely adopted in the community. Studies of the host galaxy properties and FRB position offsets from the hosts suggest that the FRB population is generally consistent with such a hypothesis (Li & Zhang 2020; Bhandari et al. 2020; Heintz et al. 2020; Bochenek et al. 2021), even though the alternative hypothesis that FRBs follow a stellar population with a significant delay with respect to star formation (e.g. the distribution of short GRBs that track binary neutron star mergers) is not ruled out

(Li & Zhang 2020). Recently, a repeating source FRB 2020120E was discovered to be located in a globular cluster of the nearby galaxy M31 (Bhardwaj et al. 2021; Kirsten et al. 2021; Nimmo et al. 2021), suggesting that at least some FRBs are associated with old stellar populations. It is desirable to know whether such a delayed population makes up a significant fraction of the entire FRB population.

So far, the FRB redshift distribution is poorly constrained. Only more than a dozen FRBs have direct redshift measurements (Tendulkar et al. 2017; Bannister et al. 2019; Ravi et al. 2019; Prochaska et al. 2019; Marcote et al. 2020; Macquart et al. 2020; Bhandari et al. 2021). These bursts were detected with a variety of radio telescopes that have very different instrumental selection effects, so this limited sample cannot give a reliable constraint on FRB redshift distribution. The dispersion measure (DM) of a FRB can be a rough proxy of its redshift, as is verified by the observational confirmation (Macquart et al. 2020) of the $DM - z$ relation long suggested theoretically (Ioka 2003; Inoue 2004; Deng & Zhang 2014). In principle, based on the observed fluence distribution, DM distribution, and inferred energy distribution of FRBs, one can constrain the redshift distribution of FRBs (Zhang et al. 2021; James et al. 2021).

However, the situation is so far inconclusive due to the small FRB samples and complicated observational selection effects. In particular, the small Parkes and ASKAP FRB samples are not inconsistent with tracking the star formation history of the universe (Zhang et al. 2021; James et al. 2021). However, models invoking a significant delay with respect to star formation (e.g. those related to binary neutron star mergers) were also found to be not inconsistent with the limited data (Zhang et al. 2021).

Recently, the CHIME/FRB Collaboration published their first FRB catalog (The CHIME/FRB Collaboration et al. 2021) reporting 536 FRBs including 62 bursts detected from 18 repeating sources. This uniform large sample provides an ideal resource to constrain the FRB redshift distribution. Chawla et al. (2021) performed a population study of the CHIME catalog. They focused on DM and scattering distributions and constrained the properties of the circumgalactic medium. They only assumed that the FRB rate evolves with redshift and tracks the star formation history of the universe without testing a range of redshift distribution models.

In this Letter, following the Monte Carlo method described in our earlier work (Zhang et al. 2021), we systematically investigate the consistency of various redshift distribution models with the CHIME FRB catalog. We find that the hypothesis that the entire FRB population track the star formation history of the universe is ruled out with high significance. We also find that the hypothesis that the FRB population tracks the accumulated stars throughout the history of the universe is also rejected. The data seem to instead approach a model that either requires the FRB sources to have a significant delay with respect to star formation or a hybrid model that includes both a dominant delayed population and an insignificant star formation population. Our method is reviewed in Section 2. The results are presented in Section 3, and conclusions are drawn in Section 4 with some discussion.

2. THE METHOD

The details of our Monte Carlo method has been described in Zhang et al. (2021). Here, we only outline the key ingredients of the method. Basically, for a uniform FRB sample detected by the same telescope (as is the case of the CHIME sample), the observed population depends on three factors: 1. the FRB isotropic energy (or luminosity) distribution, 2. the redshift distribution, and 3. the telescope’s sensitivity threshold and instrumental selection effects near the threshold.

The first factor is already well constrained from observations. The consensus (e.g. Luo et al. 2018, 2020;

Lu & Piro 2019; Lu et al. 2020; Zhang et al. 2021) is that the energy distribution of the entire FRB population is roughly a power law $dN/dE \propto E^{-\alpha}$ covering at least 8 orders of magnitude, with $\alpha \sim (1.8 - 2.0)$. There might be a high-energy exponential cutoff (Luo et al. 2020; Lu et al. 2020) but the cutoff energy E_c is not well constrained (Zhang et al. 2021)¹. The second factor is what we model in this work. The third factor is difficult to characterize. The CHIME catalog data show that the telescope specific fluence cutoff is about 0.3 Jy ms, or $\log \mathcal{F}_{\min} \simeq -0.5$ (see panel (a) of Figs. 2-5). However, due to the direction-dependent sensitivity of the telescope, there is a “gray zone” in the \mathcal{F} distribution, within which the CHIME telescope has not reached full sensitivity to all sources.

By adopting an energy (E) distribution and a redshift (z) distribution, one can simulate a large number of mock FRBs. The specific fluence of each mock burst can be calculated based on its assigned E and z values. After screening them using a telescope sensitivity model, one can finally obtain a mock “observed” sample of FRBs. Based on the DM – z relation (Deng & Zhang 2014; Zhang 2018a; Pol et al. 2019; Cordes et al. 2021)

$$\text{DM}_{\text{IGM}}(z) = \frac{3cH_0\Omega_b f_{\text{IGM}}}{8\pi Gm_p} \int_0^z \frac{(7/8)(1+z)dz}{\sqrt{\Omega_m(1+z)^3 + \Omega_\lambda}} \quad (1)$$

(where H_0 , Ω_b , Ω_m , Ω_λ are cosmological parameters whose values are adopted from the latest Planck results (Planck Collaboration et al. 2016), G is the gravitational constant, m_p is proton mass, and f_{IGM} is the fraction of baryons in the IGM, which is adopted as 0.84), one can estimate the IGM portion of the dispersion measure (DM_{IGM}) of each mock FRB. Adopting a model for the host galaxy dispersion measure (DM_{host}), one can finally simulate the excess DM distribution of the mock sample, which can be compared with the $\text{DM}_E = \text{DM}_{\text{IGM}} + \text{DM}_{\text{host}}$ data directly retrievable from the CHIME catalog (The CHIME/FRB Collaboration et al. 2021)².

¹ Even though the energy distribution was constrained from the observations using the telescopes (e.g. Parkes, ASKAP in \sim GHz) with observing band higher than that of CHIME (400 to 800 MHz), it is reasonable to assume that the *shape* of the E distribution in the CHIME band should be similar to that constrained in the GHz band. Throughout the paper, our E is defined as the isotropic energy as observed in the CHIME frequency band.

² The DM_E can be obtained by subtracting the Milky Way contribution DM_{MW} and the Milky Way halo contribution DM_{halo} from the measured DM. The former is derived from the MW electron density models NE2001 (Cordes & Lazio 2002) or YMW16 (Yao et al. 2017) and we adopt the NE2001 model throughout the paper. For the latter, we assume $\text{DM}_{\text{halo}} \sim 30 \text{ pc cm}^{-3}$ for all FRBs (e.g. Dolag et al. 2015; Prochaska & Zheng 2019).

In order to test a certain z -distribution model, we make use of three observational criteria (see Figs. 2-5): 1. the specific fluence ($\log \mathcal{F}_\nu$) distribution, 2. the isotropic energy ($\log E$) distribution, and 3. the excess dispersion measure (DM_E) distribution. The specific fluence is a convolution of the energy and redshift distributions and is insensitive to these two distributions. This is because the fluence distribution (also called $\log N - \log \mathcal{F}_\nu$ distribution) should follow a simple $N \propto \mathcal{F}_\nu^{-3/2}$ distribution regardless of the energy function if the sources are uniformly distributed in an Euclidean space³. The non-Euclidean geometry of cosmological models would break the simple scaling but only at the low fluence regime where the instrumental selection effects also become important. As a result, the criterion # 1 is most easily satisfied. For every pair of z and E distribution models, it is possible to find a sensitivity selection effect model to satisfy the $\log \mathcal{F}_\nu$ criterion. However, many models that satisfy the $\log \mathcal{F}_\nu$ distribution criterion could fail the $\log E$ and DM_E criteria. We therefore come up with the following strategy: For each z -distribution model, we will adjust the E distribution model and sensitivity model to make the \mathcal{F}_ν distribution of the mock “observed” sample to be not rejected by the Kolmogorov-Smirnov (K-S) test (all the K-S test statistics in this paper are reported with 90% confidence) against the observed \mathcal{F}_ν distribution. We then go on to evaluate the $\log E$ and DM_E distribution criteria. The model is ruled out if the same mock FRB sample fails both criteria.

In our simulations, we use the central value of DM_{host} , 107 pc cm^{-3} , as constrained from the data (e.g. Li et al. 2020)⁴. For instrumental sensitivity threshold modeling in the “gray zone”, we adopt $\log \mathcal{F}_{\nu, \text{th}}^{\min} = -0.5$ as the minimum threshold specific fluence (as shown by the data). We define a maximum threshold specific fluence $\log \mathcal{F}_{\nu, \text{th}}^{\max}$ whose value is adjusted to match the observation, and define a detection efficiency parameter η_{det} that depends on the ratio $\mathcal{R} = (\log \mathcal{F}_{\nu, \text{th}} - \log \mathcal{F}_{\nu, \text{th}}^{\min}) / (\log \mathcal{F}_{\nu, \text{th}}^{\max} - \log \mathcal{F}_{\nu, \text{th}}^{\min})$ for fluences between $\log \mathcal{F}_{\nu, \text{th}}^{\min}$ and $\log \mathcal{F}_{\nu, \text{th}}^{\max}$, such that $\eta_{\text{det}} \rightarrow 0$ at $\log \mathcal{F}_{\nu, \text{th}}^{\min}$ and $\eta_{\text{det}} \rightarrow 1$ at $\log \mathcal{F}_{\nu, \text{th}}^{\max}$. We find $\eta_{\text{det}} = \mathcal{R}^3$ can best

model the $\log \mathcal{F}_\nu$ distribution in the low-end of specific fluence distribution and therefore adopt this empirical function form in our modeling.

3. RESULTS

We investigate four families of z -distribution models in detail:

1. Star formation rate history (SFH) model: FRB sources follow the star formation history of the universe;
2. Accumulated model: FRB sources follow the number of total stars in the universe;
3. Delayed model: FRB sources follow stellar populations that have a significant delay with respect to star formation;
4. Hybrid model: A fraction of FRB sources follows star formation and another fraction follows a delayed population.

For each model, we first build a model of their redshift-dependent event rate density $dN/(dV dt)$. We then convert it to a redshift rate distribution using (e.g. Sun et al. 2015)

$$\frac{dN}{dt_{\text{obs}} dz} = \frac{1}{1+z} \frac{dN}{dt dV} \frac{dV}{dz}, \quad (2)$$

where

$$\frac{dV}{dz} = \frac{c}{H_0} \frac{4\pi D_L^2}{(1+z)^2 \sqrt{\Omega_m(1+z)^3 + \Omega_\Lambda}}, \quad (3)$$

and D_L is the luminosity distance at z . Since we only care about the z distribution, we use the normalized probability distribution functions (PDFs) of $dN/(dt dV)$ and $dN/(dt_{\text{obs}} dz)$ for all of the models, which are presented in the upper and lower panels, respectively, of Figure 1. For the data, we use only the first detected burst of each repeating FRB and the nonrepeaters.

3.1. Star formation history (SFH) model

This is the most well-motivated model. Galactic magnetars are usually believed to be young neutron stars born from supernova explosions, some of which are found to be associated with young star clusters or supernova remnants (Kaspi & Beloborodov 2017). If magnetars are the sources of most FRBs in the universe (e.g. Li & Zhang 2020; Bhandari et al. 2020; Heintz et al. 2020; Bochenek et al. 2021), one would then naturally expect that FRBs follow the star formation history of the universe (Zhang et al. 2021; James et al. 2021; The CHIME/FRB Collaboration et al. 2021).

³ This is because for a given specific burst energy and a uniform number density in space, the specific fluence is proportional to r^{-2} and the total number is proportional to r^3 ; and because such scaling relations remain the same for different burst specific energies (e.g. Zhang 2018b).

⁴ In principle, both the DM_{host} and DM_{IGM} values for individual FRBs should have a distribution around the central values. However, since we are simulating a large sample of mock FRBs, the resulting *distributions* of various parameters by adopting central values should be similar to the more realistic case involving these distributions.

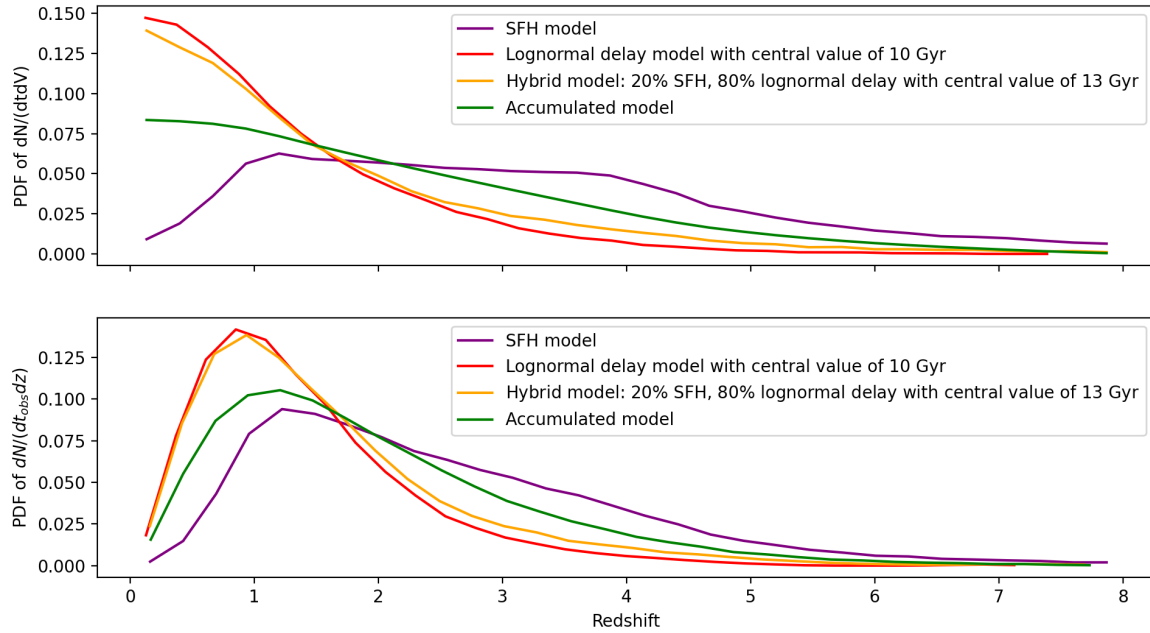


Figure 1. Probability distribution functions (PDFs) for the SFH model, lognormal delay model with a central value of 10 Gyr, hybrid model with a 20% contribution from the SFH model and 80% from a lognormal delay model a central value of 13 Gyr, and accumulated SFH model. The top panel shows the PDF of the intrinsic FRB event rate density $dN/(dt dV)$, while the bottom panel shows the PDF of the observed FRB event rate redshift distribution $dN/(dt_{\text{obs}} dz)$.

To test this model, we use the analytical three-segment empirical model of [Yüksel et al. \(2008\)](#). This model is consistent with the widely used two-segment empirical model of [Madau & Dickinson \(2014\)](#) but more precisely catches the SFH at high redshifts mapped by long gamma-ray burst observations. We assume that $dN/(dt dV)$ of FRBs is proportional to the volumetric star formation rate and derive its redshift distribution $dN/(dt_{\text{obs}} dV)$ (purple curves in Fig.1).

Even though this model was found consistent with the smaller Parkes and ASKAP FRB samples ([Zhang et al. 2021](#); [James et al. 2021](#)), Figure 2 shows that it fails to account for the CHIME data. The model overpredicts the number of FRBs at relatively high redshifts, and hence, high DM_{E} (Fig.2c), which requires an E distribution that has a higher peak than observed (Fig.2b). The K-S tests for these two criteria show very clearly that the star formation history model is rejected to describe the data. In Fig.2d, we show the two-dimensional distribution of the data and simulated mock FRBs in the $\text{DM}_{\text{E}} - \log E$ space. A deficit of low DM_{E} , low $\log E$ FRBs is clearly seen.

3.2. Accumulated model

Next, we test a z -distribution model that tracks the accumulated stars throughout history (green curves in

Fig.1). [Hashimoto et al. \(2020\)](#) advocated a model with nearly constant FRB rate during the past 10 Gyr of lookback time. They interpreted this as FRBs tracking the accumulated stellar population. We therefore test such an accumulated SFH model in detail. As shown in Fig.3, this model describes the data better than the SFH model. However, given a fluence distribution that is not rejected by the data, the resulting energy and DM_{E} distributions are still both rejected by the K-S test when tested against the data. Thus, we still reject this model to describe the CHIME FRB population. Nonetheless, since this model is a better representation of the data, it suggests that a large fraction of FRBs likely are produced by a stellar population that is significantly delayed with respect to star formation.

3.3. Delayed models

We next explore a family of models that invoke a significant delay from star formation. As described in detail in [Zhang et al. \(2021\)](#), we first generate $dN/(dt dV)$ based on the SFH model and calculate the lookback time t_L distribution of the sample. Next, we introduce a distribution model for the delay time τ , e.g. in the form of power law, Gaussian or lognormal functions (e.g. [Virgili et al. 2011](#); [Sun et al. 2015](#); [Wanderman & Piran 2015](#)). We then subtract the lookback time of the SFH model

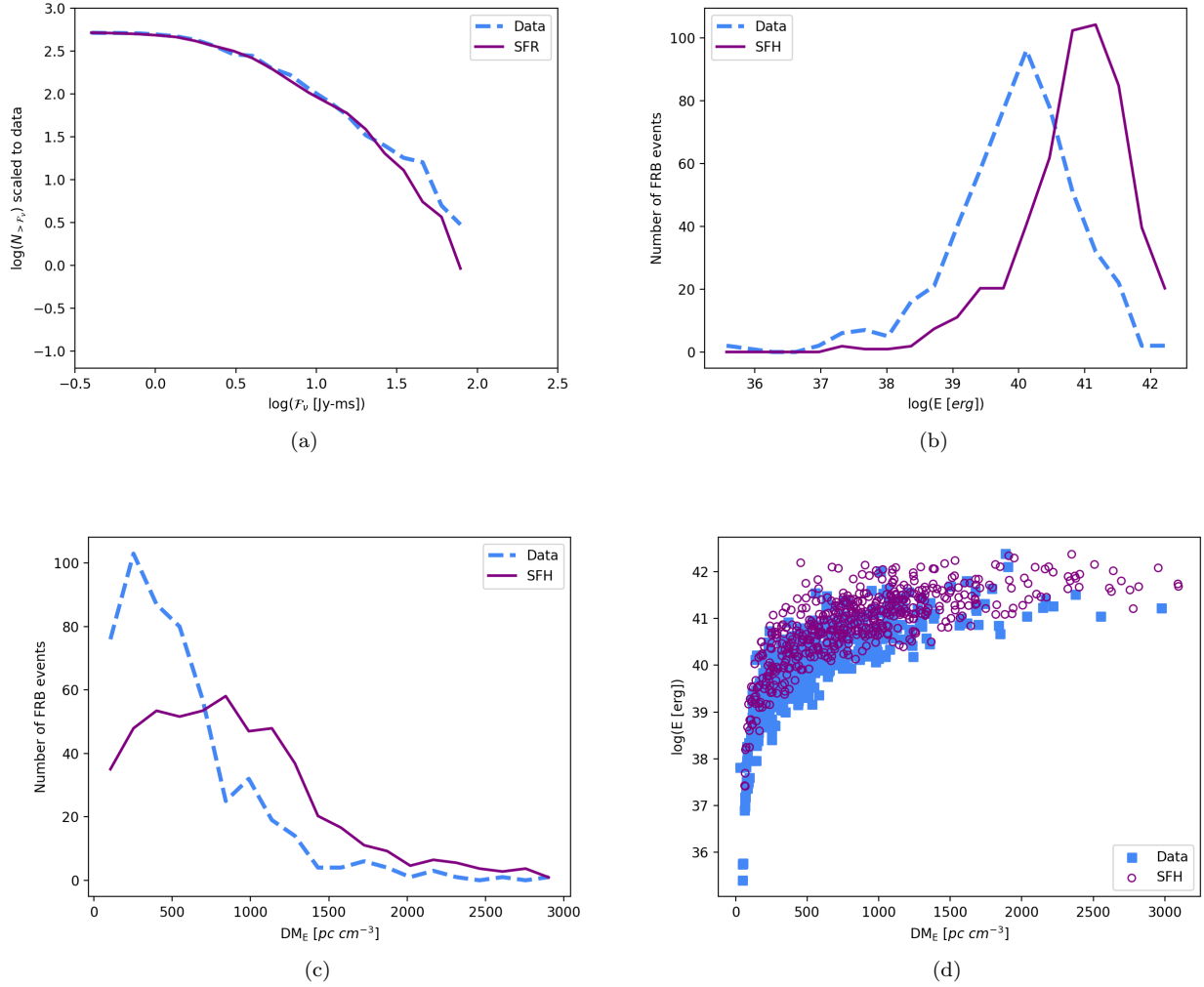


Figure 2. A test of the SFH model against the three observational criteria. The full FRB sample is tested against the model predictions. (a) The $\log N_{>F_\nu} - \log F_\nu$ test; (b) the $\log E$ distribution test, (c) the DM_E distribution test, and (d) the 2-D $DM_E - \log E$ distribution for illustrative purpose (not for testing). For panels (a), (b) and (c), the SFH simulations are scaled to the full data. For the energy distribution model, we adopt $\alpha = 1.9$ and $\log E_c = 41.5$.

by the delay time τ for each mock FRB and finally obtain the lookback time distribution of the delayed population. The cases of negative t_L are dropped out since they stand for future events. Finally, we convert the new t_L distribution to the $dN/(dt dV)$ distribution of the new model, and simulate their redshift distribution $dN/(dt_{\text{obs}} dz)$ using Eq.(2). The same approach is then applied to test the three criteria in $\log F_\nu$, $\log E$, and DM_E distributions.

Even though a family of delayed models was not rejected by the K-S test with the Parkes and ASKAP data as shown in Zhang et al. (2021), we find that all of the models previously tested (with a characteristic delay timescale of $\sim (2-3)$ Gyr and consistency with the short GRB data) are rejected by the K-S test with the CHIME

data sample. Rather, the data require a model with a much longer delay. Figure 4 (also red curves in Fig.1) presents an example of such a lognormal delay model with a central value of 10 Gyr and a standard deviation of 0.8 dex. It reproduces the data much better than the SFH model, with both the fluence and energy criteria being not rejected by the K-S test. Even though the DM_E criterion is still rejected by the K-S test, the K-S statistic is much closer to the critical value (to not reject the null hypothesis) than the SFH model. We note that there is a wide range of the inferred DM_{host} in the FRB data, which would cause more complicated features in the modeled DM_E distribution than our simple model. This could partially account for the DM_E discrepancy between our model and the data. Since there are many

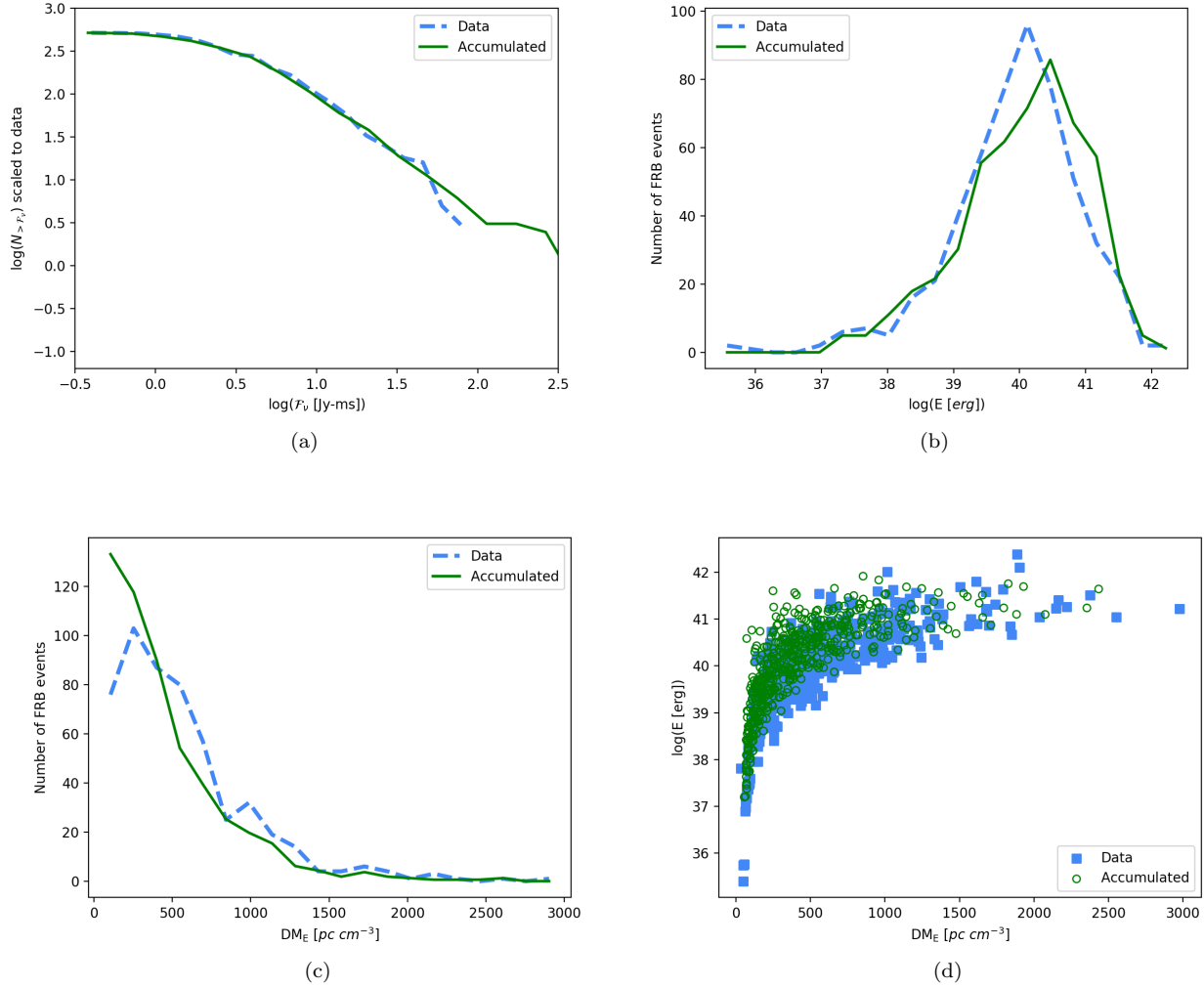


Figure 3. Similar to Figure 2, but for a test of an accumulated star formation model. All the simulations are scaled to the data. For the energy distribution model, we adopt $\alpha = 1.9$ and $\log E_c = 41$.

parameters in the model and since our goal is to test the general trend of the models rather than identify model parameters, we deem that such a significantly delayed model offers a much better description to the CHIME data than the SFH model.

3.4. Hybrid model

Finally, we test a family of models that include the mixture of a young component that tracks star formation history and an old component that has a significant delay with respect to star formation (orange curves in Fig.1). Such a model is motivated by the discoveries of the Galactic FRB 200428 (CHIME/FRB Collaboration et al. 2020; Bochenek et al. 2020), which tracks star formation, and the M81 globular cluster FRB 20200120E (Bhardwaj et al. 2021; Kirsten et al. 2021; Nimmo et al. 2021), which tracks an old population. Since the SFH model fails badly, the portion of the young population

cannot be high. To compensate the high-DM events predicted from the young population, the old population in the hybrid model needs to have an even longer delay from star formation. We test a model with a lognormal delay distribution (central value = 13 Gyr, standard deviation = 0.8 dex) of the old population that is mixed with the SFH model of the young population. The proportions are 80% for the delayed component and 20% for the SFH component. The results are shown in Figure 5. We see similar results to that of the delayed model, with the fluence and energy criteria being not rejected, but DM_E still rejected. It is clear that this model is again, a much closer model to describe the data than the SFH model. Again, since there are even more parameters in this model than the delayed model and since our goal is to test the general trend of the models, we deem that some hybrid models with a dominant delayed popula-

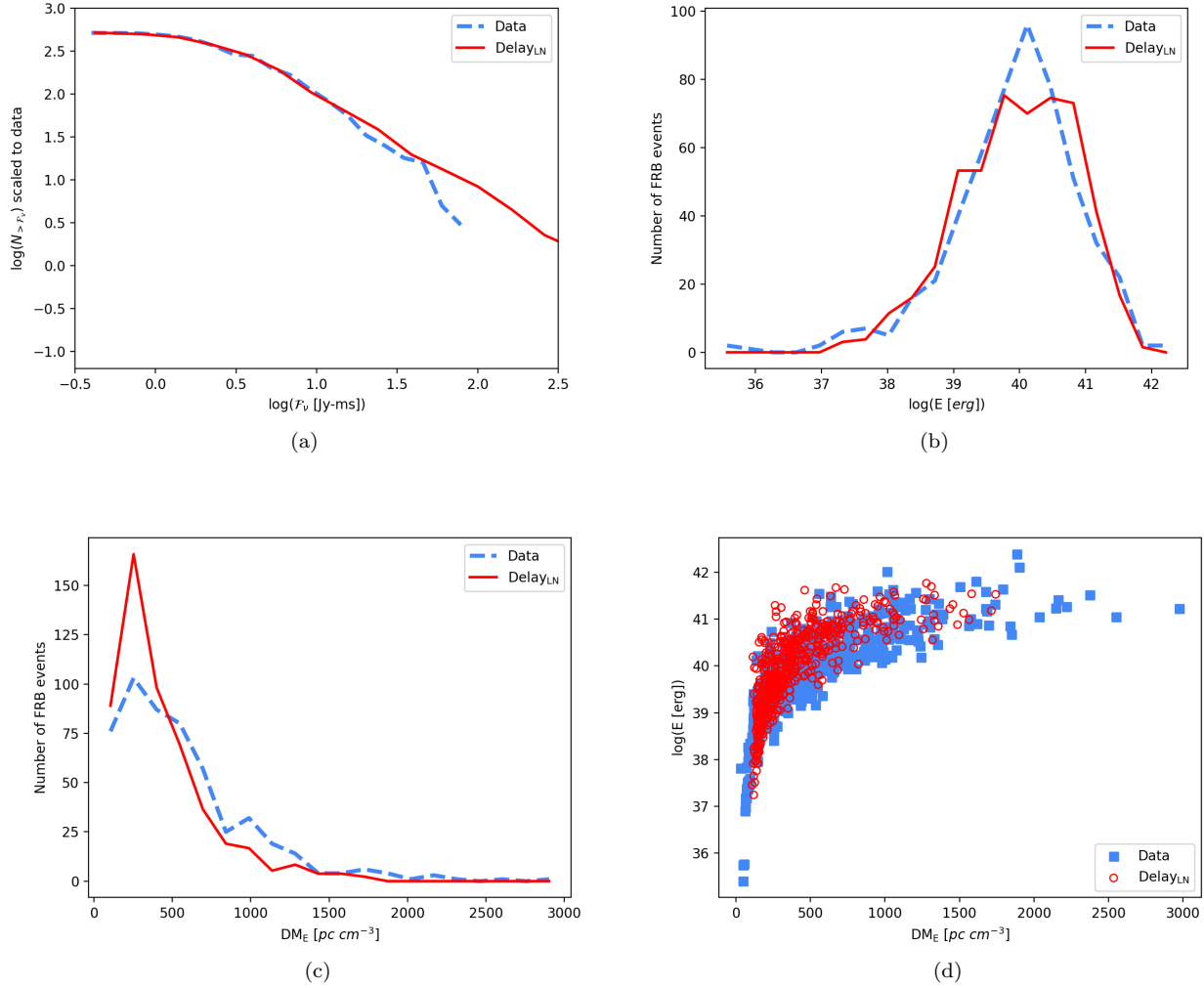


Figure 4. Similar to Figure 2, but for a test of a lognormal delay model with central value of 10 Gyr and standard deviation of 0.8 dex. All the simulations are scaled to the data. For the energy distribution model, we adopt $\alpha = 1.9$ and $\log E_c = 41$.

tion component offer a much better description to the CHIME data than the SFH model.

4. CONCLUSIONS AND DISCUSSION

Applying the Monte Carlo method developed in Zhang et al. (2021), we have systematically tested a variety of FRB redshift distribution models against the first CHIME FRB catalog data. We draw the robust conclusion that the CHIME FRB population do not track the star formation history of the universe. The hypothesis that FRBs track all the stars formed in the universe (the accumulated SFH) model, despite describing the data better, is also rejected. Instead, the models that invoke a significant delay with respect to star formation seem to be working towards the correct direction in describing the data. A model that FRBs track a population of sources that have a significant delay (~ 10 Gyr) with respect to star formation is one possibility. A hybrid

model of young and old components is another possibility, but the old population needs to be the dominant component. Even though it is difficult to pin down the parameters due to many unconstrained parameters, this general trend is quite robust. Note that the moderate delay models invoked for binary neutron star mergers (Cao et al. 2017; Zhang et al. 2021) are also not supported by the data. A much longer typical delay time is needed to match the data better.

Our results suggest that the “most conservative” scenario of FRB origin (Zhang 2020), i.e. magnetars can make them all, may have to be abandoned. Studies to interpret the M81 globular cluster FRB 20200120E (Kirsten et al. 2021; Kremer et al. 2021; Lu et al. 2021) still invoke magnetars formed from other channels other than massive star deaths, e.g. binary white dwarf mergers, accretion induced collapses, and even bi-

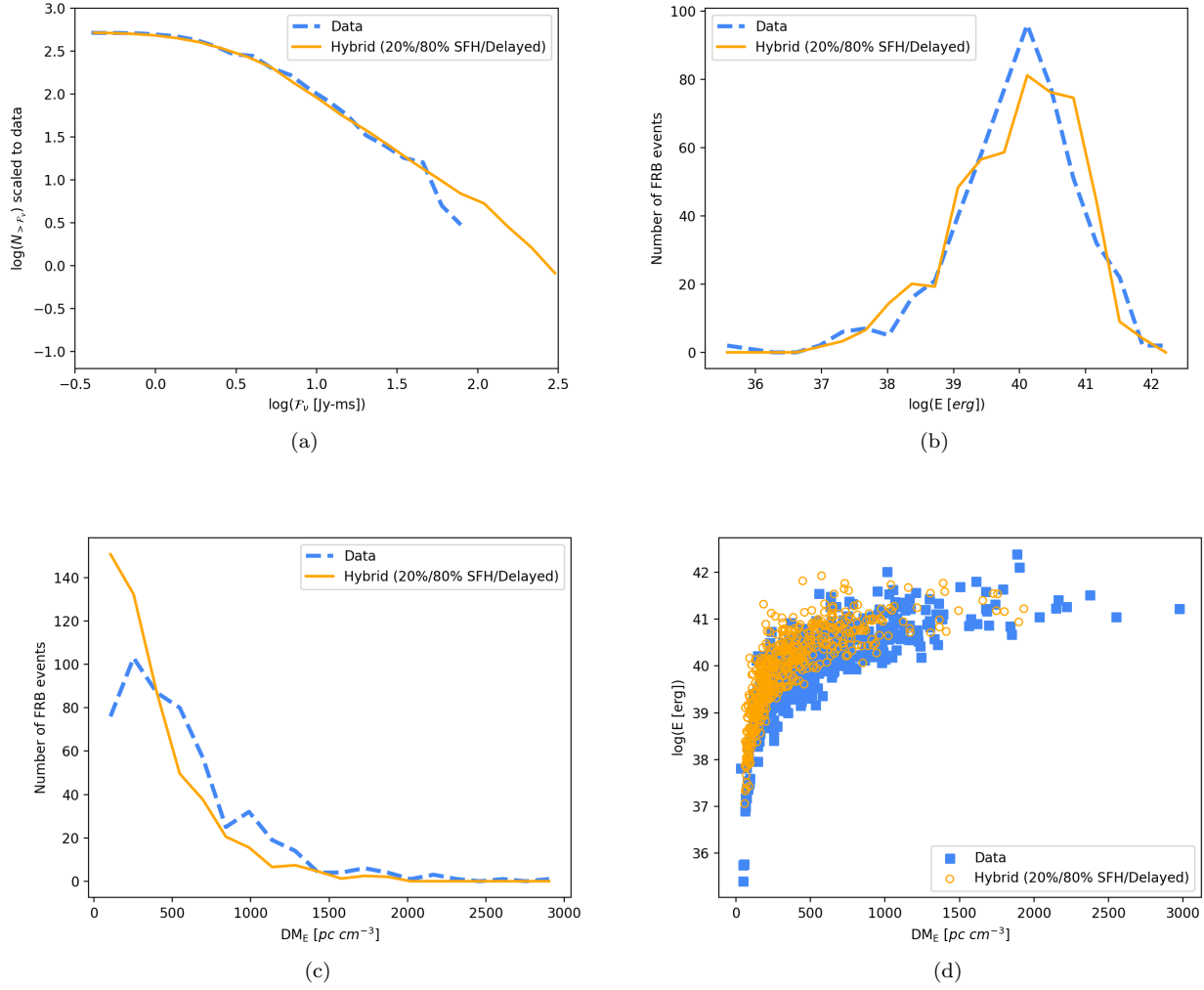


Figure 5. Similar to Figure 2, but for a test of a hybrid model that includes a young component tracking the SFH (20% of the total population) and an old component (80% of the total population) with lognormal delay with a central value of 13 Gyr and standard deviation of 0.8 dex. All the simulations are scaled to the data. For the energy distribution model, we adopt $\alpha = 1.9$ and $\log E_c = 41$.

nary neutron star mergers, to interpret FRB 20200120E. Since observationally, most known magnetars are formed from recent supernova explosions (Kaspi & Beloborodov 2017), one would expect that a small fraction of FRBs follow a delayed population if the magnetar hypothesis is correct. This is not what is inferred from the CHIME data, which requires that the delayed component is the dominant population. Challenges are raised to theorists

regarding how to make FRBs with very old stars. One possibility is that FRBs are produced by reactivation of very old neutron stars across the universe, and old magnetars may fall into such a category (e.g. Wadiasingh et al. 2020; Beniamini et al. 2020). Other possibilities, e.g. FRBs being powered by interactions with old neutron stars (Mottez & Zarka 2014; Dai et al. 2016; Zhang 2017), may also deserve reinvestigation.

REFERENCES

- Bannister, K. W., Deller, A. T., Phillips, C., et al. 2019, *Science*, 365, 565
- Beniamini, P., Wadiasingh, Z., & Metzger, B. D. 2020, *MNRAS*, 496, 3390
- Bhandari, S., Sadler, E. M., Prochaska, J. X., et al. 2020, arXiv e-prints, arXiv:2005.13160
- Bhandari, S., Heintz, K. E., Aggarwal, K., et al. 2021, arXiv e-prints, arXiv:2108.01282

- Bhardwaj, M., Gaensler, B. M., Kaspi, V. M., et al. 2021, *ApJL*, 910, L18
- Bochenek, C. D., Ravi, V., Belov, K. V., et al. 2020, *Nature*, 587, 59
- Bochenek, C. D., Ravi, V., & Dong, D. 2021, *ApJL*, 907, L31
- Cao, X.-F., Yu, Y.-W., & Dai, Z.-G. 2017, *ApJL*, 839, L20
- Chawla, P., Kaspi, V. M., Ransom, S. M., et al. 2021, arXiv e-prints, arXiv:2107.10858
- CHIME/FRB Collaboration, Andersen, B. C., Bandura, K. M., et al. 2020, *Nature*, 587, 54
- Cordes, J. M., & Lazio, T. J. W. 2002, *ArXiv Astrophysics e-prints*, astro-ph/0207156
- Cordes, J. M., Ocker, S. K., & Chatterjee, S. 2021, arXiv e-prints, arXiv:2108.01172
- Dai, Z. G., Wang, J. S., Wu, X. F., & Huang, Y. F. 2016, *ApJ*, 829, 27
- Deng, W., & Zhang, B. 2014, *ApJL*, 783, L35
- Dolag, K., Gaensler, B. M., Beck, A. M., & Beck, M. C. 2015, *MNRAS*, 451, 4277
- Hashimoto, T., Goto, T., On, A. Y. L., et al. 2020, *MNRAS*, 498, 3927
- Heintz, K. E., Prochaska, J. X., Simha, S., et al. 2020, arXiv e-prints, arXiv:2009.10747
- Inoue, S. 2004, *MNRAS*, 348, 999
- Ioka, K. 2003, *ApJL*, 598, L79
- James, C. W., Prochaska, J. X., Macquart, J. P., et al. 2021, arXiv e-prints, arXiv:2101.07998
- Kaspi, V. M., & Beloborodov, A. M. 2017, *ARA&A*, 55, 261
- Kirsten, F., Marcote, B., Nimmo, K., et al. 2021, arXiv e-prints, arXiv:2105.11445
- Kremer, K., Piro, A. L., & Li, D. 2021, *ApJL*, 917, L11
- Li, C. K., Lin, L., Xiong, S. L., et al. 2021, *Nature Astronomy*, 5, 378
- Li, Y., & Zhang, B. 2020, *ApJL*, 899, L6
- Li, Z., Gao, H., Wei, J. J., et al. 2020, *MNRAS*, arXiv:2004.08393
- Lu, W., Beniamini, P., & Kumar, P. 2021, arXiv e-prints, arXiv:2107.04059
- Lu, W., Kumar, P., & Zhang, B. 2020, *MNRAS*, 498, 1397
- Lu, W., & Piro, A. L. 2019, *ApJ*, 883, 40
- Luo, R., Lee, K., Lorimer, D. R., & Zhang, B. 2018, *MNRAS*, 481, 2320
- Luo, R., Men, Y., Lee, K., et al. 2020, *MNRAS*, 494, 665
- Macquart, J. P., Prochaska, J. X., McQuinn, M., et al. 2020, *Nature*, 581, 391
- Madau, P., & Dickinson, M. 2014, *ARA&A*, 52, 415
- Marcote, B., Nimmo, K., Hessels, J. W. T., et al. 2020, *Nature*, 577, 190
- Mereghetti, S., Savchenko, V., Ferrigno, C., et al. 2020, *ApJL*, 898, L29
- Mottez, F., & Zarka, P. 2014, *A&A*, 569, A86
- Nimmo, K., Hessels, J. W. T., Kirsten, F., et al. 2021, arXiv e-prints, arXiv:2105.11446
- Planck Collaboration, Ade, P. A. R., Aghanim, N., et al. 2016, *A&A*, 594, A13
- Pol, N., Lam, M. T., McLaughlin, M. A., Lazio, T. J. W., & Cordes, J. M. 2019, *ApJ*, 886, 135
- Prochaska, J. X., & Zheng, Y. 2019, *MNRAS*, 485, 648
- Prochaska, J. X., Macquart, J.-P., McQuinn, M., et al. 2019, *Science*, 366, 231
- Ravi, V., Catha, M., D’Addario, L., et al. 2019, *Nature*, 572, 352
- Ridnaia, A., Svinkin, D., Frederiks, D., et al. 2021, *Nature Astronomy*, 5, 372
- Sun, H., Zhang, B., & Li, Z. 2015, *ApJ*, 812, 33
- Tavani, M., Casentini, C., Ursi, A., et al. 2021, *Nature Astronomy*, 5, 401
- Tendulkar, S. P., Bassa, C. G., Cordes, J. M., et al. 2017, *ApJL*, 834, L7
- The CHIME/FRB Collaboration, :, Amiri, M., et al. 2021, arXiv e-prints, arXiv:2106.04352
- Virgili, F. J., Zhang, B., O’Brien, P., & Troja, E. 2011, *The Astrophysical Journal*, 727, 109
- Wadiasingh, Z., Beniamini, P., Timokhin, A., et al. 2020, *ApJ*, 891, 82
- Wanderman, D., & Piran, T. 2015, *MNRAS*, 448, 3026
- Yao, J. M., Manchester, R. N., & Wang, N. 2017, *ApJ*, 835, 29
- Yüksel, H., Kistler, M. D., Beacom, J. F., & Hopkins, A. M. 2008, *ApJL*, 683, L5
- Zhang, B. 2017, *ApJL*, 836, L32
- . 2018a, *ApJL*, 854, L21
- . 2018b, *The Physics of Gamma-Ray Bursts*, doi:10.1017/9781139226530
- . 2020, *Nature*, 587, 45
- Zhang, R. C., Zhang, B., Li, Y., & Lorimer, D. R. 2021, *MNRAS*, 501, 157